Computers & Structures Vol. 31, No. 1, pp. 73–80, 1989
Printed in Great Britain.

0045-7949/89 $3.00 + 0.00

FINITE ELEMENT ANALYSIS OF COUPLED THERMOELASTICITY

J. P. CARTER and J. R. BOOKER
School of Civil and Mining Engineering, University of Sydney, NSW 2006, Australia

Abstract—Most thermal stress analyses assume that the determination of the temperature field is uncoupled from that of the stress and displacement fields, while assuming that the stress and displacement fields depend on the temperature field. This semi-coupled approach to thermoelasticity is not entirely consistent. In this paper the governing equations for the fully coupled theory of thermoelasticity are developed and a method for solving these equations, based on the finite element technique, is proposed. The numerical method is used to obtain approximate solutions which are then compared with analytical solutions to a number of test problems. An assessment is also made of the importance of the full coupling. The use of the solution technique is further illustrated with some example problems from geotechnical engineering.

1. INTRODUCTION

There are a number of significant problems in engineering requiring thermal stress analysis. An important class of problems arises in mechanical engineering and includes the analysis of machine components subjected to high temperature environments and large temperature variations such as in a turbine. Problems of this type have been solved in the past using the semi-coupled theory of thermoelasticity (e.g. [1]). In this approach, it is assumed that the temperature changes induce thermal strains and if the body is restrained then transient stress changes will accompany these strains. Furthermore, it has been usual to assume that strains arising from boundary loadings and body forces induce only small temperature changes in the material, and hence may conveniently be ignored. Analyses of this type are traditionally carried out in two stages. The temperature distribution is first determined (by solution of the governing Laplace or diffusion equations) and this is then used to calculate the response of the elastic body to the imposed thermal gradients and other applied forces. It has generally been considered that this approximate, semi-coupled approach is satisfactory when applied to materials like metals. It remains to be shown whether this approach is sufficiently accurate for other engineering materials, particularly the more exotic composites that have been manufactured in recent times and geological materials, i.e. soil and rock.

In geotechnical engineering most analysis is restricted to isothermal conditions, but there exists a number of important problems that require an analysis of thermal effects. Examples include the disposal of radioactive waste and mining in hot rocks. For these cases knowledge of the thermal properties of the geological materials is less precise than for metals, and at this stage it is difficult to be sure whether the traditional, semi-coupled approach to thermal analysis will be adequate. For this reason a fully coupled approach to the problem has been adopted in this paper. The governing equations for the fully coupled theory are developed and a finite element solution scheme is suggested. Numerical results have been obtained for several problems for which it is possible to obtain analytical solutions, thus providing a means of assessing the accuracy of the numerical solutions. A parametric study of these problems has been carried out to determine when full coupling of the thermal and elastic processes is important. To illustrate the utility of this approach, results are also obtained for two problems encountered in geotechnical engineering, viz. the heat flow into a square tunnel during cooling of its surfaces and the storage of hot radioactive waste in a borehole.

2. GOVERNING EQUATIONS

The physical process of coupled thermoelastic deformation is governed by the following set of equations.

2.1. *Equilibrium*

In the absence of body forces, equilibrium of the body is expressed, in a Cartesian coordinate system, as

$$\partial^{\mathrm{T}}\boldsymbol{\sigma} = 0 \tag{1}$$

in which

$$\boldsymbol{\sigma}^{\mathrm{T}} = (\sigma_x, \sigma_y, \sigma_z, \tau_{xy}, \tau_{yz}, \tau_{zx})$$

and

$$\partial^{\mathrm{T}} = \begin{bmatrix} \partial/\partial x & 0 & 0 & \partial/\partial y & 0 & \partial/\partial z \\ 0 & \partial/\partial y & 0 & \partial/\partial x & \partial/\partial z & 0 \\ 0 & 0 & \partial/\partial z & 0 & \partial/\partial y & \partial/\partial x \end{bmatrix}$$

$\boldsymbol{\sigma}$ is the vector of stress components, with tensile normal stress regarded as positive. These quantities represent the increase over the initial state of stress due to the applied loading and the temperature change.

2.2. *Strain–displacement relations*

These relations may be expressed in matrix form as

$$\boldsymbol{\epsilon} = \partial \mathbf{u} \tag{2}$$

where $\boldsymbol{\epsilon}^{\mathrm{T}} = (\epsilon_x, \epsilon_y, \epsilon_z, \gamma_{xy}, \gamma_{yz}, \gamma_{zx})$ is the vector of strain components, and $\mathbf{u}^{\mathrm{T}} = (u_x, u_y, u_z)$ is the vector of displacement components.

2.3. *Constitutive law*

For the case of thermoelastic deformations, Hooke's law for an isotropic material may be written as

$$\boldsymbol{\sigma} = -\beta\theta\mathbf{a} + D\boldsymbol{\epsilon} \tag{3}$$

in which $\theta = T - T_0$,

$$\mathbf{a}^{\mathrm{T}} = (1, 1, 1, 0, 0, 0).$$

T_0 and T represent the constant initial and current absolute temperatures, respectively, θ represents the temperature change and D is a matrix of elastic constants, given by

$$D = \begin{bmatrix} \lambda+2G & \lambda & \lambda & 0 & 0 & 0 \\ & \lambda+2G & \lambda & 0 & 0 & 0 \\ & & \lambda+2G & 0 & 0 & 0 \\ & & & G & 0 & 0 \\ & & & & G & 0 \\ \text{symmetric} & & & & & G \end{bmatrix}$$

with λ and G the Lamé modulus and elastic shear modulus of the material, respectively. The thermal stress modulus, β, is given by

$$\beta = E\alpha/(1-2\nu) \tag{4}$$

where E and ν are Young's modulus and Poisson's ratio of the material and α is the coefficient of linear thermal expansion.

2.4. *Conservation of energy*

If complete coupling of the elastic and thermal processes is considered, then the condition for conservation of mechanical and thermal energy at any point can be written in integral form as

$$-\int_0^t \nabla^{\mathrm{T}}\mathbf{h}^{\mathrm{T}}\,\mathrm{d}t = \rho c_v\theta + T\beta\epsilon_v \tag{5}$$

in which

$\mathbf{h}^{\mathrm{T}} = (h_x, h_y, h_z)$ = the heat flux,
ρ = the mass density,
c_v = the specific heat (at constant volume),
ϵ_v = the volume strain,
$\nabla^T = (\partial/\partial x, \partial/\partial y, \partial/\partial z)$ = the gradient operator,

and where the thermoelastic deformations of interest occur during the time interval 0 to t.

The term $T\beta\epsilon_v$ accounts for the mechanical energy involved in the coupled process and in the more conventional uncoupled analysis this term is ignored. In the present case the temperature changes considered will be small compared to the ambient absolute temperature ($\theta \ll T_0$), and thus to sufficient accuracy T may be approximated by the constant T_0 in eqn (5).

2.5. *Heat flow*

The conduction of heat through the solid body is governed by the Fourier law, viz.

$$\mathbf{h} = -k\nabla\theta \tag{6}$$

in which k is the thermal conductivity.

3. VIRTUAL WORK

In the absence of any increase in body force the equation of virtual work, relating the internal strain energy to the work done by the surface tractions $\mathbf{F}$, can be written as,

$$\int \delta\boldsymbol{\epsilon}^{\mathrm{T}}\boldsymbol{\sigma}\,\mathrm{d}V - \int \delta\mathbf{u}^{\mathrm{T}}\mathbf{F}\,\mathrm{d}S = 0 \tag{7}$$

where $\delta\mathbf{u}$ represents a virtual displacement field consistent with the displacement boundary conditions and $\delta\boldsymbol{\epsilon}$ represents the associated virtual strains.

If the boundary points are either insulated or subjected to a specified temperature, and the virtual temperature field, $\delta\theta$, is consistent with these conditions, then the following equation must be satisfied:

$$\int \delta\theta\left[\rho c_v\theta + \beta T_0\epsilon_v - \int_0^t \nabla^{\mathrm{T}}\mathbf{h}\,\mathrm{d}t\right]\mathrm{d}V = 0. \tag{8}$$

Substitution of eqn (6) into (8) gives

$$\int\left[\delta\theta\left(\frac{c_v\rho}{T_0}\right)\theta + \delta\theta\beta\epsilon_v + \int_0^t\left[\nabla^T\delta\theta\left(\frac{k}{T_0}\right)\nabla\theta\,\mathrm{d}t\right]\right]\mathrm{d}V = 0. \tag{9}$$

The incorporation of specified flux boundary conditions into eqn (9) is relatively straightforward but is not pursued here.

4. FINITE ELEMENT SOLUTION

An approximate solution of the governing equations presented above may be obtained by application of the finite element method of spatial discretization.

Suppose that the continuous values of $\mathbf{u}$ and θ can be represented adequately by their values at selected nodes, i.e.,

$$\mathbf{u} = N\boldsymbol{\delta} \tag{10}$$

and

$$\theta = X\boldsymbol{\varphi} \tag{11}$$

where $\boldsymbol{\delta}$ and $\boldsymbol{\varphi}$ are the vectors containing the nodal values and N and X contain the shape functions of the displacements and temperature, respectively.

The strain components now may be written as

$$\boldsymbol{\epsilon} = B\boldsymbol{\delta} \tag{12}$$

where $B = \partial N$, and the temperature gradients can be expressed as

$$\nabla\theta = Y\boldsymbol{\varphi} \tag{13}$$

where $Y = \partial^T \mathbf{a} X$.

When eqns (10)–(12) and the extended form of Hooke's law (3) are substituted into eqn (7), it is found that

$$K\boldsymbol{\delta} - L\boldsymbol{\varphi} = \mathbf{b} \tag{14}$$

where $K = \int B^T D B \, dV$,

$L = \int Z^T \beta X \, dV$,

$Z = \mathbf{a}^T B$,

and $\mathbf{b}$ is a vector of nodal forces corresponding to the applied surface tractions.

Substitution of eqns (10)–(13) into (9) gives

$$-L^T\boldsymbol{\delta} - M\boldsymbol{\varphi} - \int_0^t \Phi\boldsymbol{\varphi}\, dt = 0 \tag{15}$$

where

$$\Phi = \int \mathbf{Y}^T\left(\frac{k}{T_0}\right)\mathbf{Y}\, dV$$

and

$$M = \int \mathbf{X}^T\left(\frac{\rho c_v}{T_0}\right)\mathbf{X}\, dV.$$

The solution of eqns (14) and (15) is obtained using a time-marching procedure as follows. For the thermoelastic material assumed here, the material properties are independent of stress level, temperature and time, so that matrices K, L, M and Φ contain only constant terms. Equation (15) may be written incrementally and for the time interval $t - \Delta t$ to t it takes the form,

$$-L^T\Delta\boldsymbol{\delta} - M\Delta\boldsymbol{\varphi} - \int_{t-\Delta t}^{t} \Phi\boldsymbol{\varphi}(t)\, dt = 0 \tag{16}$$

where $\Delta\boldsymbol{\delta} = \boldsymbol{\delta}(t) - \boldsymbol{\delta}(t - \Delta t)$,

$\Delta\boldsymbol{\varphi} = \boldsymbol{\varphi}(t) - \boldsymbol{\varphi}(t - \Delta t)$.

To sufficient accuracy the time integral may be evaluated numerically, so that (16) may be written as

$$-L^T\Delta\boldsymbol{\delta} - M\,\Delta\boldsymbol{\varphi} - f\,\Delta t\Phi\,\Delta\boldsymbol{\varphi} = \Delta t\Phi\boldsymbol{\varphi}(t - \Delta t) \tag{17}$$

where $0 \leqslant f \leqslant 1$. Therefore the incremental solution is determined from the system of equations

$$\begin{bmatrix} K & -L \\ -L^T & -M - f\Delta t\Phi \end{bmatrix} \cdot \begin{bmatrix} \Delta\boldsymbol{\delta} \\ \Delta\boldsymbol{\varphi} \end{bmatrix} = \begin{bmatrix} \Delta\mathbf{b} \\ \Delta t\Phi\boldsymbol{\varphi}(t - \Delta t) \end{bmatrix}. \tag{18}$$

The solution over the full time range of interest is obtained by incrementing the time and successively solving equations of the type given in (18). For stability of the time marching scheme f must be greater than or equal to one-half [2], and often it is convenient to select $f = 1$.

5. COMPARISON OF NUMERICAL AND CLOSED-FORM SOLUTIONS

The formulation presented in the previous sections has been encoded in a general purpose finite element program called AFENA [3]. This program was used on a microcomputer to calculate the results for the following test problems.

5.1. *One-dimensional transient heat flow*

This problem is defined in Fig. 1. A layer of thermoelastic material of thickness h is initially at a uniform absolute temperature of T_0 throughout. The

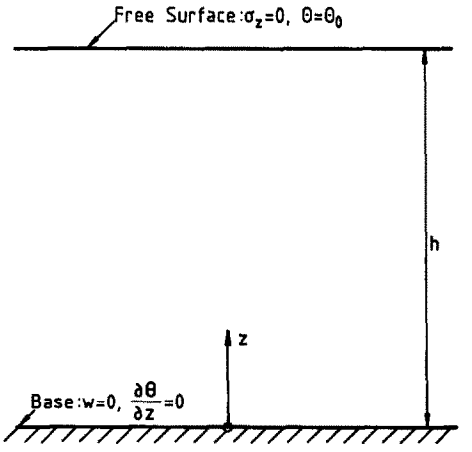

Fig. 1. One-dimensional problem.

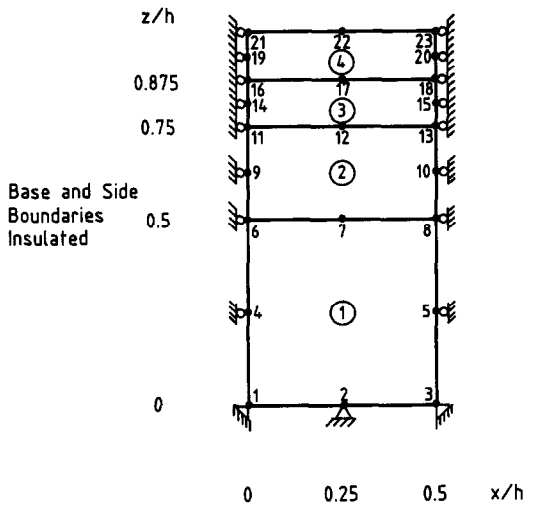

Fig. 2. F.E. mesh used for one-dimensional problem.

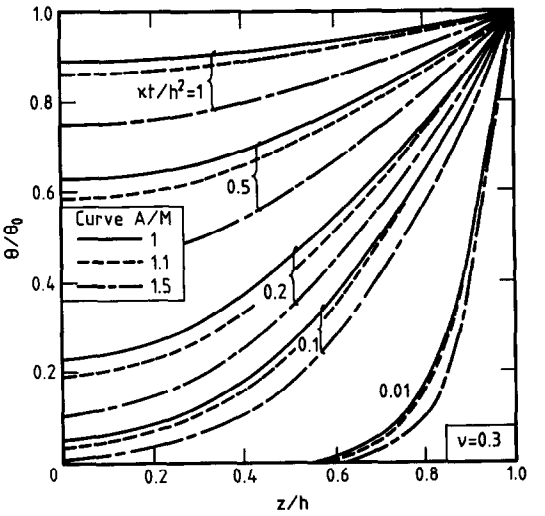

Fig. 3. Temperature isochrones for one-dimensional heat flow.

base of the layer ($z = 0$) is rigid (vertical displacement, $w = 0$) and insulated ($\partial\theta/\partial z = 0$) and for $t > 0$ the temperature of the unstressed surface is maintained at an absolute value of $T = T_0 + \theta_0$; i.e. the temperature increase at the surface is θ_0. The time-dependent response of the layer has been calculated analytically, as well as numerically, using the mesh depicted in Fig. 2.

It can be shown that the exact solution for this problem is

$$\bar{\theta} = \left(\frac{\theta_0}{s}\right)\frac{\cosh[\mu z]}{\cosh[\mu h]} \tag{19}$$

and

$$\bar{w} = \left(\frac{\theta_0}{\mu s}\right)\left(\frac{\beta}{M}\right)\frac{\sinh[\mu z]}{\cosh[\mu h]} \tag{20}$$

where

$$\mu = \sqrt{(sA/\kappa M)}. \tag{21}$$

In the above equations $\bar{\theta}$ and $\bar{w}$ are the Laplace transforms of the temperature change and vertical displacement, respectively. A and M are the constrained moduli corresponding to adiabatic and isothermal conditions, κ is the thermal diffusivity, and s is the Laplace transform variable. For isothermal conditions M is related to Young's modulus, E, and Poisson's ratio, v, by

$$M = \frac{E(1-v)}{(1+v)(1-2v)}. \tag{22}$$

It may be shown that the adiabatic modulus, A, is given by

$$A = M + \beta^2 T_0/(\rho c_v) \tag{23}$$

where β, c_v and ρ have been defined previously. The thermal diffusivity is related to the other material properties by

$$\kappa = k/(\rho c_v). \tag{24}$$

To obtain the quantities θ and w, the transforms $\bar{\theta}$ and $\bar{w}$ must be inverted. The inversion process is relatively easy when carried out numerically using the efficient scheme developed by Talbot [4]. In addition, the case corresponding to $A = M$ is simply one-dimensional diffusion, the solution for which is well known.

Analytical solutions for the isochrones of temperature change and for the variation of the surface heave are plotted in Figs 3 and 4. These curves demonstrate the influence of the parameter A/M on the coupled heat flow; the case where $A = M$ corresponds to uncoupled thermoelastic behaviour. It can be seen that the coupling of the thermal and elastic processes

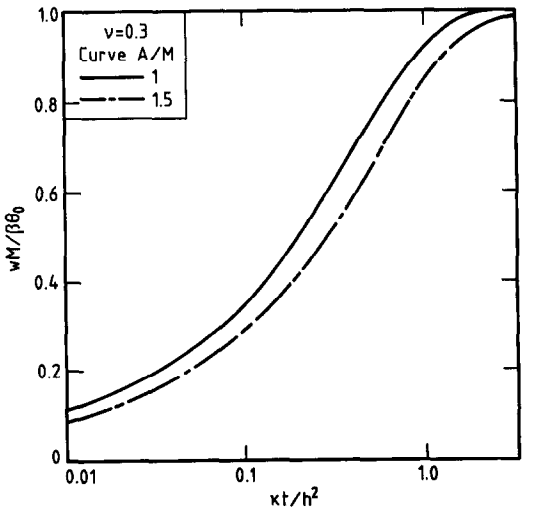

Fig. 4. Surface heave for one-dimensional heat flow.

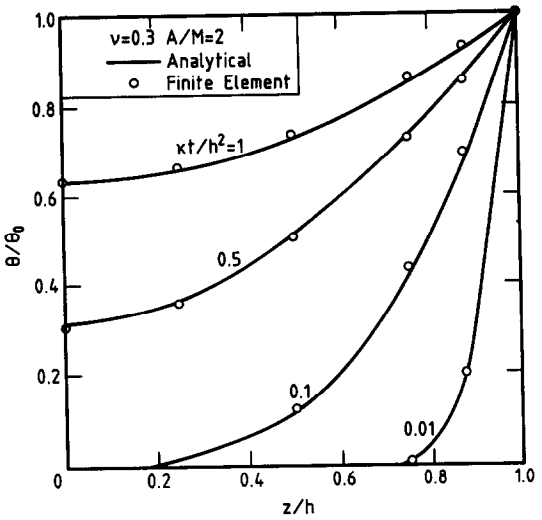

Fig. 5. Comparison of predicted temperature isochrones.

is significant for a material with $A/M = 1.5$. This is likely to be an upper limit on the modulus ratio for many of the more conventional engineering materials.

The accuracy of the finite element formulation and coding was validated by comparing the analytical and numerical solutions for a material with $A/M = 2$. Although in many cases this is likely to be an unrealistic choice of the modulus ratio, it does allow a comparison for a case where coupling effects are particularly significant. As can be seen from Figs 5 and 6, the agreement between the analytical and numerical solutions is very satisfactory.

5.2. *Transient heat flow in an infinite cylinder*

The problem defined in Fig. 7 is now considered. Initially the infinitely long cylinder was at a uniform absolute temperature T_0. At time $t = 0^+$ the temperature of its unstressed outer surface ($r = a$) was raised to $T = T_0 + \theta_0$ and thereafter held constant. The

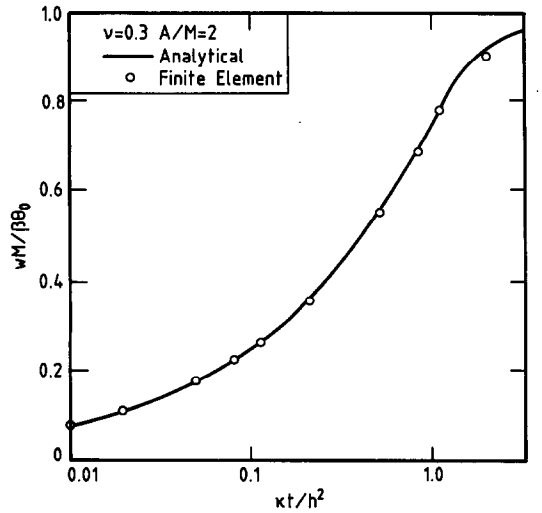

Fig. 6. Comparison of predictions of surface heave.

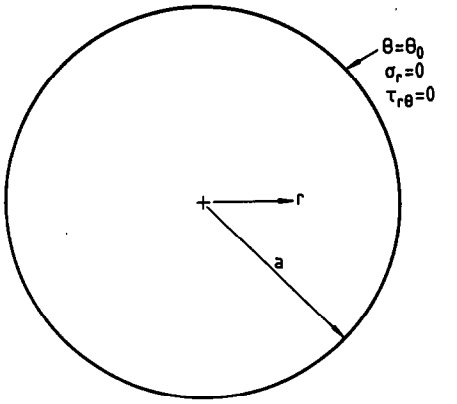

Fig. 7. Infinite cylinder with zero initial temperature, thereafter $\theta = \theta_0$ at $r = a$.

diffusion of heat into the cylinder and the associated, coupled thermoelastic deformations have been calculated both analytically and numerically with the mesh shown in Fig. 8.

The exact solution for this problem can be written as

$$\beta\bar{\theta} = 2(M - A)R + SI_0[\mu r] \tag{25}$$

$$\frac{\bar{u}}{r} = R + \left(\frac{S}{M}\right)\left(\frac{I_0'[\mu r]}{\mu r}\right) \tag{26}$$

where

$$R = \left(\frac{G}{M}\right)\left(\frac{I_0'[\mu a]}{\mu a}\right)\Omega,$$

$$S = (A - G)\Omega,$$

$$\Omega = \beta\bar{\theta}_0 \Big/ \left[(A - G)I_0[\mu a] + 2(M - A)\left(\frac{G}{M}\right)\left(\frac{I_0'[\mu a]}{\mu a}\right)\right]$$

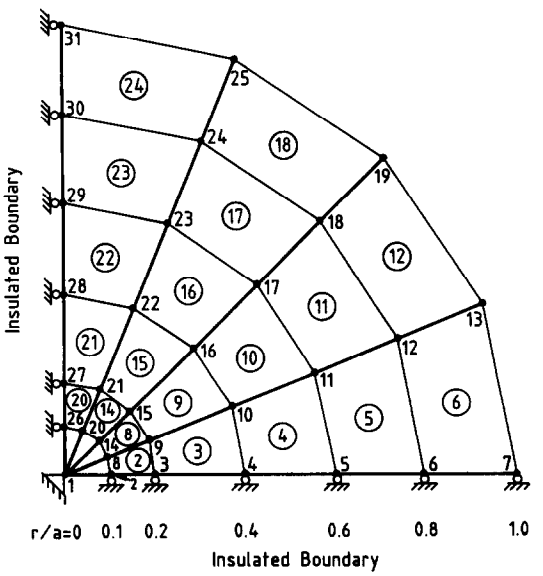

Fig. 8. F.E. mesh used for cylinder problem.

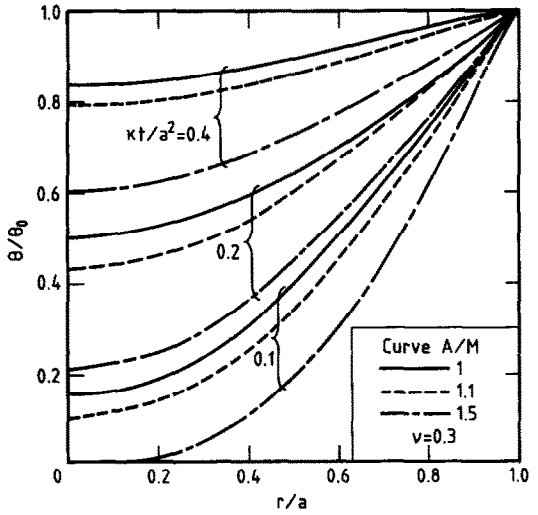

Fig. 9. Temperature isochrones for radial heat flow in a cylinder.

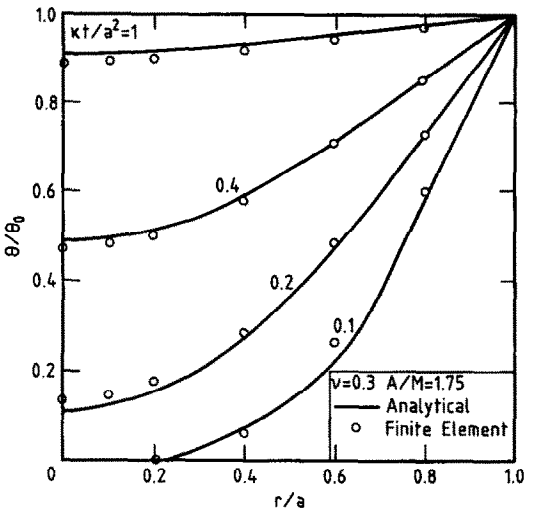

Fig. 11. Comparison of predicted temperature isochrones.

and I_0 is the modified Bessel function of zero order and u denotes the radial displacement. As before, the transforms are most easily inverted numerically using the scheme devised by Talbot [4], to give the temperature change θ and the radial displacement u. In addition, the case where $A = M$ corresponds to radial diffusion and the solution is well known (e.g. [5], p. 198).

The analytical solutions have been evaluated for typical values of the modulus ratio A/M and the results have been plotted in Figs 9 and 10. As in the previous example, the curves indicate that the coupling of the thermal and elastic processes is significant for larger values of the ratio A/M. The numerical solutions have been compared with the analytical results in Figs 11 and 12 where it is demonstrated that satisfactory agreement has been achieved.

6. GEOTECHNICAL EXAMPLES

The effectiveness of the numerical technique is further illustrated with the analysis of two problems of practical significance in geotechnical engineering.

6.1. *Cooling of a square tunnel*

Consider a long, deep, square-sectioned tunnel of side $a = 3.5$ m, penetrating a thermoelastic rock mass. The rock mass is assumed to be homogeneous and isotropic and to have properties as defined in Fig. 13. Initially the rock is at a uniform temperature of 50°C. At time $t = 0$, the temperature of the tunnel walls is reduced by 30°C to 20°C and for time $t > 0$, heat will be extracted through the rock surface and the deformations of the surrounding mass will be time-dependent. This type of problem will arise in practice when an underground roadway is cooled,

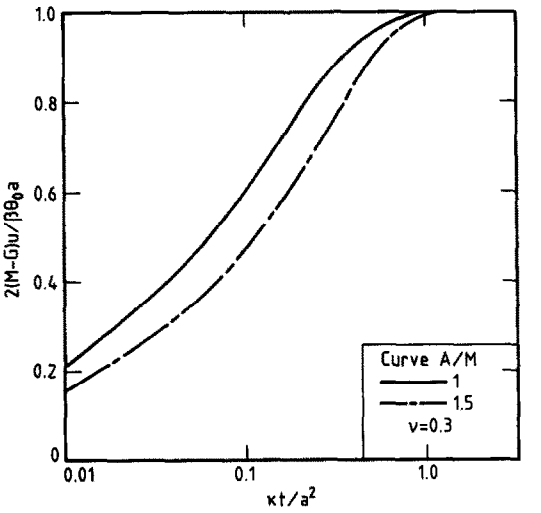

Fig. 10. Radial expansion of a heated elastic cylinder.

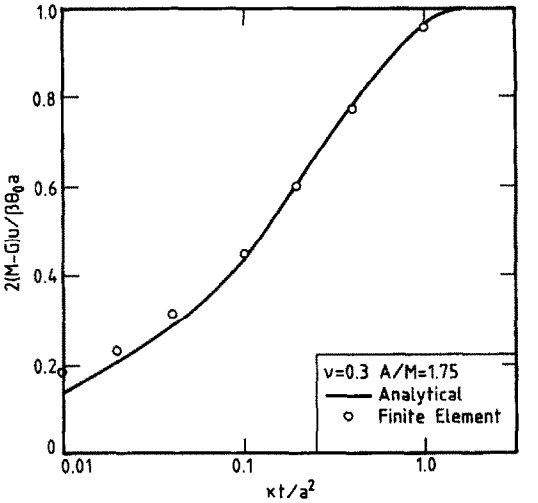

Fig. 12. Comparison of predictions of radial expansion of a heated cylinder.

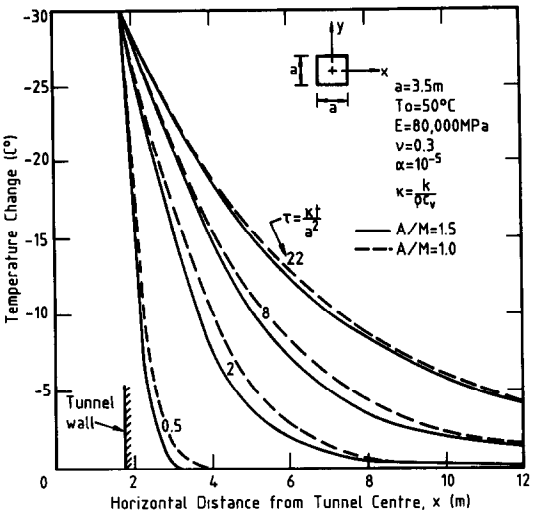

Fig. 13. Isochrones of temperature change on the horizontal mid-plane of a square tunnel.

e.g. in a deep mine. At depth the rock temperatures will be higher than the surface temperatures because of the existence of the geothermal gradient, and cooling will be required to allow men and machines to work at these depths while winning ore.

The problem described above has been solved using the finite element scheme and some numerical results are given in Fig. 13. Isochrones of temperature change on the horizontal plane at mid-height of the tunnel are shown, and the figure also indicates the significance of a fully coupled analysis by showing curves for $A/M = 1$ and 1.5. It can be seen from Fig. 13 that coupling tends to retard slightly the diffusion of heat through the rock mass. However, it can be noted that the coupling implied by $A/M = 1.5$ has little influence on the transient stress distributions in this problem.

6.2. *Heat flow from a borehole*

The problem of the disposal of radioactive wastes is currently being tackled by the nuclear industry. Various schemes for the long term storage of these wastes have been proposed and one of these involves the placement of cannisters of waste in deep boreholes in stable geological deposits.

An important aspect of the storage problem concerns the generation of heat by the decaying radioactive waste materials and the effect of this heat on the surrounding rock masses. Heat will be generated for a significant period of time after initial placement and thus predictions of the transient thermal response of the soil or rock masses are required.

A typical problem of heat generation within a deep cylindrical borehole is considered here. As the hole is deep and the continuous depth interval in which the cannisters are placed is long, conditions of plane strain are assumed and thus the field quantities will vary only in the radial direction. Finite element computations have been made of the transient response of a rock mass for which $E = 80{,}000$ MPa, $\nu = 0.3$, $\alpha = 10^{-5}\,°C^{-1}$ and $\kappa = 0.02\,m^2$/year. The temperature boundary condition at the wall of the borehole ($r = a$) is assumed to vary with time. In particular, the temperature is considered to increase initially linearly with time, until it reaches a maximum increase of 50°C after 2 years. Thereafter, the boundary temperature reduces exponentially with time, so that 50 years after initial placement of the waste it will drop to an overall increase of 25°C. These boundary conditions at $r = a$, can be summarized as follows:

$$\theta_a = 25t, \qquad 0 \leqslant t \leqslant 2 \text{ years}$$

$$= 50\exp(0.0288 - 0.0144t), \quad t \geqslant 2 \text{ years}.$$

Numerical predictions of the transient thermoelastic response of the rock mass are summarized in Figs 14–16. Figure 14 shows the temperature distributions at selected times, viz. $t = 2$, 22 and 222 years after initial placement of the heat source. Isochrones at 2 and 22 years have been plotted for rock masses for which $A/M = 1$ and 1.5, i.e. predictions using the semi-coupled and fully coupled theories are given. It can be seen that the fully coupled theory predicts a slightly slower flow of heat away from the borehole and into the rock mass. Only one curve has been plotted for $t = 222$ years, because the differences between predictions for $A/M = 1$ and 1.5 cannot be detected at the scales used in Figs 14–16.

The transient stress changes are shown in Figs 15 and 16, with compression plotted here as positive. Figure 15 indicates that the radial stress changes are entirely compressive and it is interesting that these stresses continue to increase for some time after $t = 2$ years, even though the boundary temperature is decreasing for $t > 2$ years. These stress increases occur as the heat is redistributed within the rock

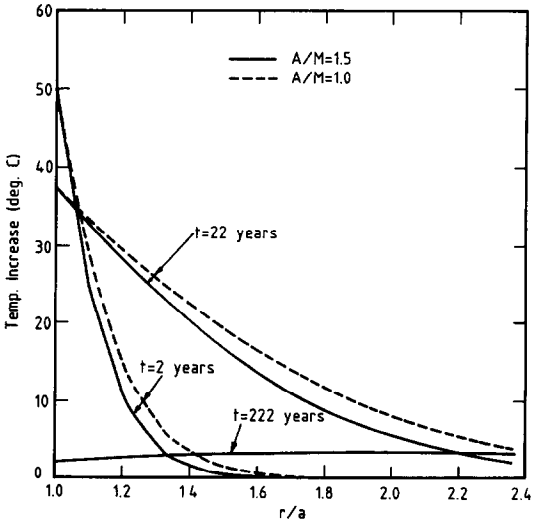

Fig. 14. Temperature isochrones for the borehole problem.

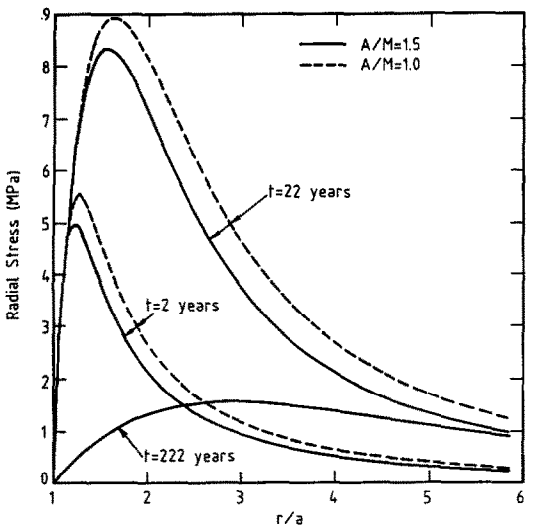

Fig. 15. Isochrones of radial stress change for the borehole problem.

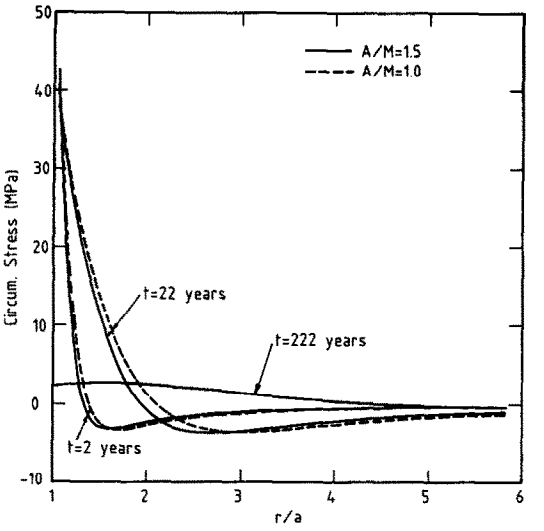

Fig. 16. Isochrones of circumferential stress change for the borehole problem.

mass. Eventually the radial stresses close to the hole decrease, as can be seen, for example, at $t = 222$ years.

The stress changes in the circumferential direction are plotted in Fig. 16 and it is notable that very high compressive stress changes (in excess of 30 MPa) are induced in the rock close to the borehole wall. At larger radii, e.g. for $r/a \geqslant 1.5$, significant tensile stress changes are induced in the circumferential direction at $t = 2$ and 22 years. At the later time $t = 222$ years the circumferential stress changes are relatively small and compressive. Of course, at large times the predicted stress changes become infinitesimal.

It is also interesting to note that the fully coupled theory predicts significant but not large differences in the stress distributions, compared to those obtained using the semi-coupled approach. Indeed, it is likely that for most geological materials A/M < 1.5, and so the semi-coupled theory should adequately predict the thermoelastic response.

7. CONCLUSIONS

The theory of fully coupled thermoelasticity has been presented, together with a numerical solution scheme based on the use of the finite element technique with a time-marching strategy. This procedure has allowed the solution for the full transient response in thermoelastic problems. Solutions obtained numerically have been compared with analytical solutions and the agreement was found to be satisfactory. An examination was made of the significance of full coupling on the predicted response of the thermoelastic material for a number of initial value problems. It has been demonstrated that coupling has a significant influence on the rate of heat diffusion throughout the material whenever the adiabatic and isothermal moduli (A and M, respectively) are sufficiently different, say by about 25 per cent or more. It is expected that many natural materials will have ratios of A to M less than 1.25 and so the traditional, semi-coupled theory may provide sufficient accuracy in most geotechnical problems. However, it seems likely that the fully coupled theory may have application to the prediction of the thermomechanical behaviour of modern composite materials, although specific data on their thermal and elastic properties are not available at present to fully justify this assertion.

Acknowledgement—The authors wish to acknowledge the value of discussions with D. W. Smith during the preparation of this paper.

REFERENCES

1. A. Nowacki, *Thermoelasticity*, Pergamon Press, International Series of Monographs in Aeronautics and Astronautics (1962).
2. J. R. Booker and J. C. Small, An investigation of the stability of numerical solutions of Biot's equations of consolidation. *Int. J. Solids Struct.* **11**, 907–917 (1975).
3. J. P. Carter, *AFENA—A Finite Element Numerical Algorithm—Users' Manual*. School of Civil and Mining Engineering, University of Sydney, Australia (1986).
4. A. Talbot, The accurate numerical inversion of Laplace transforms. *J. Inst. Math. Applic.* **23**, 97–120 (1979).
5. H. S. Carslaw and J. C. Jaeger, *Conduction of Heat in Solids* (2nd Edn, Paperback). Clarendon Press, Oxford, U.K. (1986).